



Turning Bacteria Suspensions into Superfluids

Héctor Matías López,¹ Jérémie Gachelin,² Carine Douarche,³ Harold Auradou,^{1,*} and Eric Clément²

¹Université Paris-Sud, CNRS, F-91405, Lab FAST, Bâtiment 502, Campus Univ, Orsay F-91405, France

²Physique et Mécanique des Milieux Hétérogènes (UMR 7636 ESPCI/CNRS/Université P.M. Curie/Université Paris-Diderot),
10 rue Vauquelin, 75005 Paris, France

³Laboratoire de Physique des Solides, Université Paris-Sud, CNRS UMR 8502, F-91405 Orsay, France

(Received 19 March 2015; revised manuscript received 24 May 2015; published 7 July 2015)

The rheological response under simple shear of an active suspension of *Escherichia coli* is determined in a large range of shear rates and concentrations. The effective viscosity and the time scales characterizing the bacterial organization under shear are obtained. In the dilute regime, we bring evidence for a low-shear Newtonian plateau characterized by a shear viscosity decreasing with concentration. In the semidilute regime, for particularly active bacteria, the suspension displays a “superfluidlike” transition where the viscous resistance to shear vanishes, thus showing that, macroscopically, the activity of pusher swimmers organized by shear is able to fully overcome the dissipative effects due to viscous loss.

DOI: 10.1103/PhysRevLett.115.028301

PACS numbers: 83.80.Hj, 47.57.Qk, 82.70.Kj, 83.80.Lz

Owing to its relevance in medicine and ecology and its importance for technological applications, the hydrodynamics of active suspensions is at the center of many recent fundamental studies [1,2]. In nature, wide classes of living microorganisms move autonomously in fluids at very low Reynolds numbers [3]. Their motility stems from a variety of propulsive flagellar systems powered by nanomotors. For bacteria such as *Bacillus subtilis* or *E. coli*, the propulsion comes from the rotation of helix-shaped flagella creating a propulsive force at the rear of the cell body [4]. Consequently, many original fluid properties stem from the swimming activity [5–11]. Because of hydrodynamic interactions, bacteria may produce mesoscopic patterns of collective motion sometimes called “bioturbulence” [12–17]. In a flow, these bacteria may organize spatially [18], and under shear, for pusher swimmers, the swimming activity yields the possibility to decrease the macroscopic viscosity to values below the suspending fluid viscosity [5]. In the dilute regime, kinetic theories via a simple account of the dominant long range hydrodynamic field [19–22] provide closed forms for shear viscosity as a function of shear rate. Remarkably, at a low shear rate, these theories predict a Newtonian plateau with a viscosity decreasing linearly with concentration [19–21]. On the other hand, phenomenological theories were also proposed to describe macroscopically active suspensions via a coupling of hydrodynamic equations with polar and/or nematic order parameters [2,5,6,23–25]. A striking outcome of these theories is that, for a set of coupling parameters rendering essentially a high swimming activity, a self-organized motive macroscopic flow may show up in response to shear [23–25]. This onset of a dissipationless current is described in analogy with the superfluidity transition [23,24] of liquids. Experimental evidence for viscosity reduction to values below the suspending fluid viscosity

was brought for *B. subtilis* [8] and *E. coli* [26] suspensions. However, no viscosity vs shear rate and vs time under steady and uniform shear exists. Moreover, these pioneering experiments did not provide evidence for the low-shear viscous plateau which is at the core of all theoretical predictions in the dilute regime. Finally, the phenomenological predictions for the nonlinear regime have remained so far unobserved. Noticeably, for unicellular algae, viewed as “puller” swimmers, the predicted low-shear rate increase of viscosity was measured experimentally [9]. In this Letter, in addition to a viscosity vs shear rate and vs time characterization of an *E. coli* suspension, we provide, in the dilute regime and at a low shear rate, experimental evidence for a linear decrease of the apparent viscosity with bacteria concentration. We also explore regimes of higher concentration and describe the conditions where we observe a transition to a dissipation-free macroscopic flow.

The active fluids considered here are prepared out of two strains of wild type *E. coli* (ATCC9637 and RP437) suspended into a minimal medium where the bacteria are still motile but do not divide. ATCC9637 is cultured overnight at 25 °C in LB medium shaken at 240 rpm. RP437 is cultured overnight at 30 °C and shaken at 240 rpm in M9 minimal medium supplemented with 1 mg/ml casamino acids and 4 mg/ml glucose. Next, the culture is washed twice by centrifugation (2300 g for 10 min), and the cells are resuspended into a motility medium containing 10 mM potassium phosphate pH 7.0, 0.1 mM K-EDTA, 34 mM K-acetate, 20 mM sodium lactate, and 0.005% polyvinylpyrrolidone (PVP-40). To avoid bacterial sedimentation, the suspension is mixed with Percoll (1 vol/1 vol). The bacteria concentration n is represented by its volume fraction $\phi = n/V_b$, where V_b is the bacteria body volume chosen as the classical value $V_b = 1 \mu\text{m}^3$.

Shear stress is measured in a low-shear Couette rheometer (Contraves 30) designed especially for probing low-viscosity fluids. The inner bob (radius $R_i = 5.5$ mm, length 8 mm, and underside cone angle 20°) is suspended by a torsion wire into a cup (inner radius $R_o = 6$ mm). The cup rotates at an angular rate Ω controlled by a computer. The corresponding shear rate is $\dot{\gamma} = (\Omega R_o / R_o - R_i)$ and is given with a precision of 0.5%. The central feature, making this instrument very precise for low stress measurements, is that the central bob is kept fixed by a feedback counter-rotation of the suspending wire. The instrument measures the compensating torque required to keep the torsion wire at its null position. The torque is then converted into shear stress every 0.7 s with a sensitivity of 10^{-3} mPa.

Importantly, due to the small surface area between the fluid and the air, the flux of O_2 is insufficient to compensate the amount of O_2 consumed by the bacterial activity. To avoid bacteria suffocation and, consequently, a severe drop

of activity, we supplement the suspension with L-serine, an amino acid allowing the bacteria to keep a significant swimming activity in the absence of oxygen [27,28]. Therefore, in the early instants of the measurements, the bacteria are still in oxygenated conditions, but, since they consume the oxygen, their mean velocity and diffusion coefficient decrease and stabilize within about 10 min. Consequently, we observe a continuous increase in the suspension viscosity until a constant value is reached. Then, by metabolizing L-serine, bacteria sustain a constant activity lasting for a few hours (see Supplemental Material [29]). To obtain a full rheogram as displayed in Fig. 1(b), the following protocol is used. A volume (1.25 ml) of the suspension is poured into the rheometer's cup, and then the bob is set into place. After 30 s of rest, the cup is rotated for 30 s at a steady state shear rate. The rotation is then stopped for 30 s. These steps are repeated with increasing shear rate values. Once the highest $\dot{\gamma}$ is reached, the procedure is

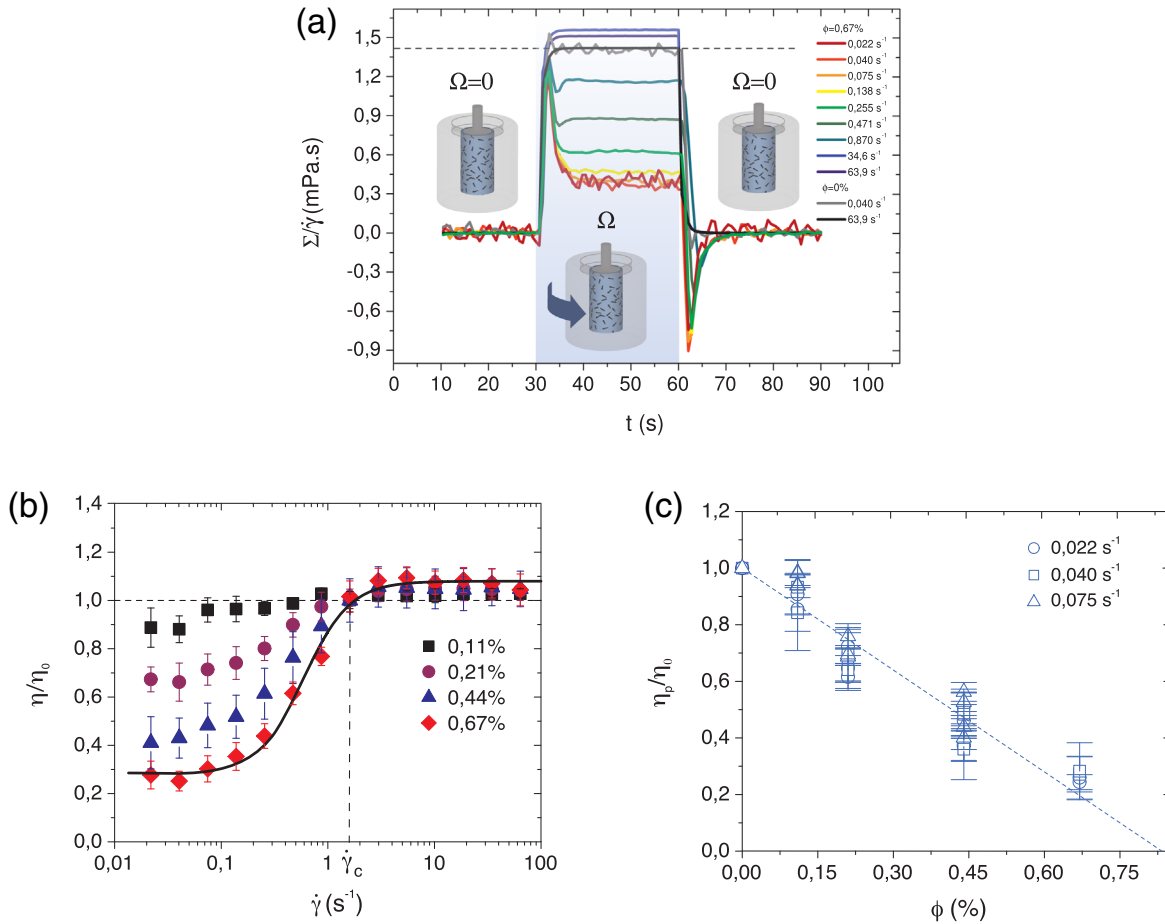


FIG. 1 (color online). Shear stress response for an *E. coli* suspension (ATCC9637 strain, $T = 25^\circ\text{C}$). (a) Shear stress Σ rescaled by the applied shear rate $\dot{\gamma}$ during the rotation to display an effective viscosity $\Sigma/\dot{\gamma}$ in the sheared regime. Gray and black lines: Fluid without bacteria ($\phi = 0$). Colored solid lines: Fluid with bacteria ($\phi = 0.67\%$). Various $\dot{\gamma}$ are applied ranging from 64 (dark blue line) down to 0.022 s⁻¹ (dark red line). (b) Relative viscosity η/η_0 averaged over three realizations as a function of $\dot{\gamma}$ (empty square, $\phi = 0.11\%$; empty circle, $\phi = 0.21\%$; empty triangle, $\phi = 0.44\%$; empty diamond, $\phi = 0.67\%$). The solid line is an adjustment by the Carreau law: $\eta/\eta_0 = 1.08 - 0.795/[1 + (\dot{\gamma}/0.6)^2]$. The vertical dashed line shows $\dot{\gamma}_c$; below this shear rate $\eta(\dot{\gamma})/\eta_0$ is less than 1. (c) Values of the plateau viscosity η_p/η_0 as functions of the bacteria volume fraction ϕ for very low shear rates (empty circle, $\dot{\gamma} = 0.022$ s⁻¹; empty square, $\dot{\gamma} = 0.04$ s⁻¹; empty triangle, $\dot{\gamma} = 0.075$ s⁻¹).

repeated in decreasing order to verify the reversibility of the viscous response.

Rheology measurements were first performed to obtain viscosity at volume fractions between $\phi = 0.1\%$ and 0.67% . In Fig. 1(a), we display the stress responses obtained for a suspension at a given ϕ , for various shear rates. For the suspending fluid alone (a Newtonian fluid, $\eta_0 = 1.4 \text{ mPa} \cdot \text{s}$), stress-time responses, at the start or at the stop of the applied shear, are fast and correspond to the device compliance (gray and black lines). A similar behavior is observed for the suspensions probed at high shear rates which moreover display a viscosity higher than η_0 as observed classically for suspensions of passive particles. However, at low shear rates, a strikingly different behavior is observed. When shear starts, the stress jumps to the value measured in the absence of bacteria, and then,

after an exponential decrease, lasting for a few seconds, a steady effective viscosity— η —is reached. When shear stops, the stress decreases abruptly and eventually changes sign. Finally, the stress relaxes exponentially to 0 with a characteristic time τ_r^- not very different from the time scale τ_r^+ , needed to reach a steady viscous response under shear [data in Fig. 2(c)]. In this last stage, the bacterial motion induces a motive stress on the inner bob.

Figure 1(b) shows the suspension viscosity η as a function of $\dot{\gamma}$ for different volume fractions ranging from $\phi = 0.11\%$ (1.1×10^9 bact/mL) up to $\phi = 0.67\%$ (6.7×10^9 bact/mL). We observe the three regimes predicted by the theories [19,20], (i) at high shear rates ($\dot{\gamma} > 1 \text{ s}^{-1}$), the active contribution to viscosity is negligible and a Newtonian plateau appears akin to suspensions of passive particles of the same shape; (ii) below a critical

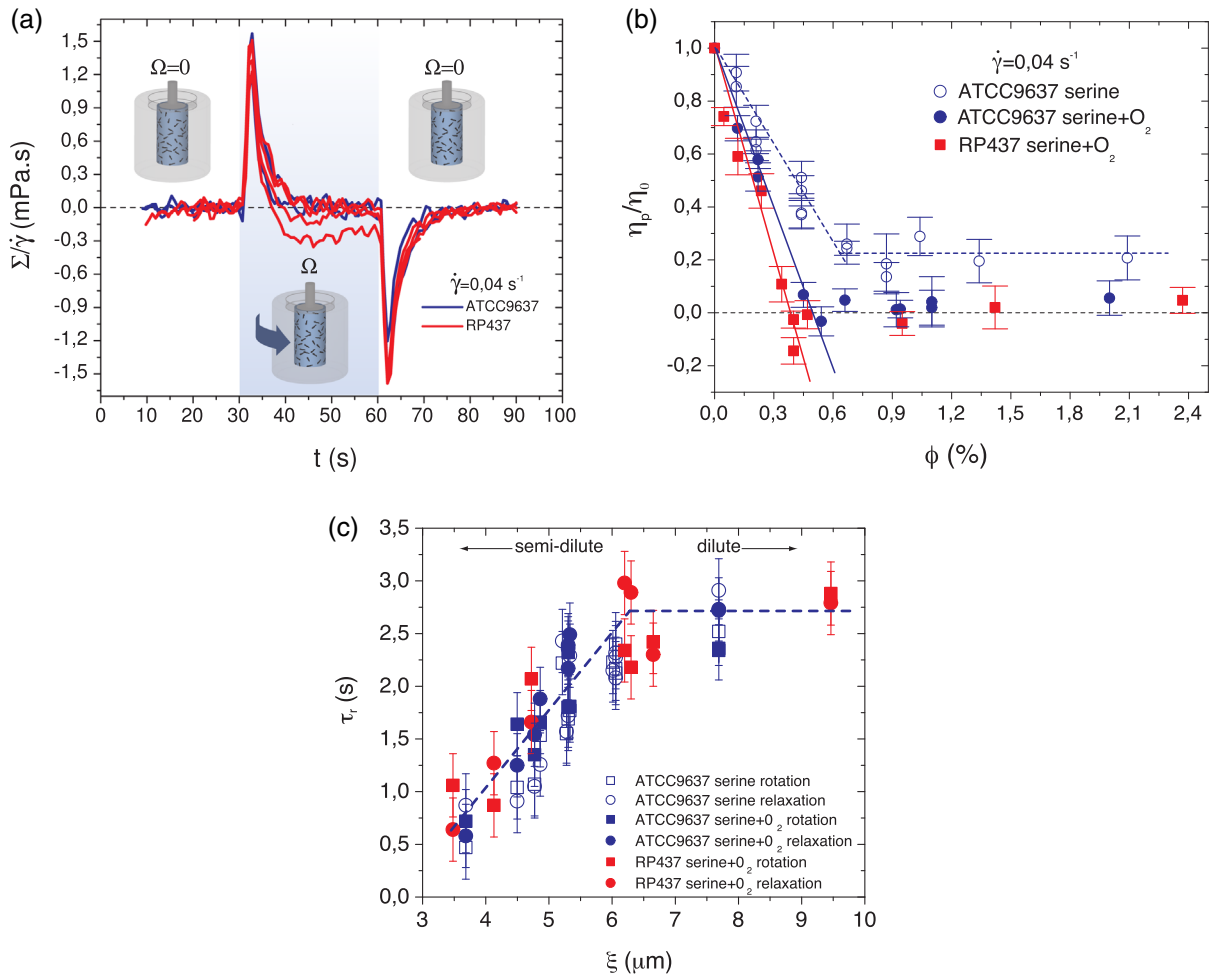


FIG. 2 (color online). (a) Shear stress response Σ rescaled by the shear rate $\dot{\gamma}$ for the ATCC9637 strain (blue lines) and RP437 strain (red lines). All experiments are performed with $\dot{\gamma} = 0.04 \text{ s}^{-1}$. In some cases, the stress response can reach negative values. (b) Variation of the viscosity η_p/η_0 as a function of the volume fraction of bacteria ϕ in oxygenated conditions (filled symbols) and deoxygenated conditions (empty symbols). Dashed lines are meant as guides only. (c) Relaxation time τ_r , obtained by adjusting exponentially the stress relaxation at the start of the shear (rotation) and at the end of the shear (relaxation) as a function of the mean distance ($\xi = \phi^{-1/3}$) between bacteria (empty symbols, deoxygenated conditions; filled symbols, oxygenated conditions; blue symbols, ATCC9637 strain; red symbols, RP437 strain).

shear rate value $\dot{\gamma}_c \leq 1.5 \text{ s}^{-1}$, the suspension viscosity is lower than the suspending fluid viscosity; (iii) at low shear rates ($\dot{\gamma} \leq 0.1 \text{ s}^{-1}$), an “active viscous plateau” $\eta_p(\phi)$ appears. Furthermore, the theories also predict a linear dependance of η_p with ϕ given by

$$\frac{\eta_p}{\eta_0} = 1 + K \left(\frac{\tau}{t_c} \right) \phi, \quad (1)$$

where $K \propto [A - B(\tau/t_c)]$; t_c is the time taken by a bacterium to drag the fluid over its size, and τ characterizes the directional persistence of a swimming trajectory [30]; A and B depend solely on the bacterium shape [19–22]. As shown in Fig. 1(c), $\eta_p(\phi)$ decreases linearly with the concentration as $\eta_p/\eta_0 = 1 + K\phi$ with $K \simeq -120 \pm 10$, as long as the shear rate is sufficiently low (i.e., in the range $0.022\text{--}0.075 \text{ s}^{-1}$). The experimental results are very consistent with active suspension theories for pusher swimmers in the dilute regime. Noticeably, within the framework of closed form theories established in the dilute regime, such a complete determination of the viscous response can be used to give an estimation of the microscopic bacterial activity (see [29] for an explicit derivation of the dipolar strength and other microscopic parameters via the Saintillan [20] kinetic model).

We next compare the viscous response of the bacteria for two different activity levels. When both O_2 and L-serine are present in the suspension, one obtains an “hyperactivated” regime characterized by high values of bacteria diffusivity and swimming velocity ($D = 7 \times 10^{-11} \text{ m}^2/\text{s}$ and $V_0 = 28 \mu\text{m}/\text{s}$ for ATCC9637). After 10 min, when O_2 is consumed, the motility is maintained by the metabolization of L-serine. In this case, one has a lower activity with $D = 1.2 \times 10^{-11} \text{ m}^2/\text{s}$ and $V_0 = 20 \mu\text{m}/\text{s}$ (see [29], Fig. 2). The first regime only lasts a few minutes, and the measurements were thus restricted to a single $\dot{\gamma}$ sufficiently low (here 0.04 s^{-1}) to estimate η_p , the active plateau viscosity. In the “hyperactive” domain, η_p is again found for $\phi < 0.6\%$ to decrease linearly with ϕ but with a larger slope $K' \simeq -200 \pm 3$ [see Fig. 2(b)]. This result demonstrates that the slope K is strongly related to the bacterial activity. Next, these experiments were repeated with the second *E. coli* strain (RP437). These bacteria have a lower swimming velocity $V_0 = 20 \mu\text{m}/\text{s}$ and also a slightly longer body length $2.2 \mu\text{m}$ instead of $1.7 \mu\text{m}$. A linear η_p vs ϕ relation is also found but with a larger negative slope $K'' \sim -259 \pm 13$ [red squares in Fig. 2(b)], demonstrating a correlation between the bacterial characteristics and the rheological response at a low shear rate.

We finally increase the number of bacteria in the solution to values above 0.6% . For the ATCC9637 strain in a medium that does not contain oxygen [empty symbols in Fig. 2(b)], we observe that the viscosity becomes constant and independent of ϕ for $\phi > 0.7\%$ with $\eta_p/\eta_0 \sim 0.2$. In

oxygenated conditions and for highly motile batches, we measure that the viscosity η_p/η_0 also reaches a constant value beyond $\phi \sim 0.5\%$ and $\phi \sim 0.4\%$ for ATCC9637 and RP437, respectively. For the three cases, the active plateau viscosity becomes thus independent of the concentration over a significant domain (from $\phi = 0.6\%$ up to 2.4%). In addition under hyperactivated conditions, one observes a viscous response reaching zero [see Fig. 2(a)], meaning that the local viscous dissipation is macroscopically entirely compensated by the swimming activity. Moreover, with the very active RP strain, negative values for η_p [see Figs. 2(a) and 2(b)] could be obtained at the edge of the transition. To validate the existence and robustness of this low viscosity regime, other experiments at lower shear rate and higher temperature were conducted: They all display a $\eta \sim 0$ regime. These results point towards the idea of an organization process triggered by the shear flow which may last even when the shear ceases. In Fig. 2(c), we plot the relaxation times τ_r^+ and τ_r^- as functions of the mean distance $\xi (= \phi^{-1/3})$ between bacteria. The transition between the dilute and the semidilute regimes occurs here for a distance $\xi \simeq 6 \mu\text{m}$. In fact, below this length, the relaxation time is found to decrease linearly with ξ (while the viscosity η_p remains constant). The result seems to be consistent with the phenomenological picture proposed for an active polar swimmer and with the clustering interaction recently observed in the absence of flow [16] and suggests that the collective effect becomes important for distances shorter than $6 \mu\text{m}$.

In conclusion, our experiments show that the bacterial activity has a measurable influence on shear viscosity. We brought direct experimental evidence, at low shear rates, for an active viscous plateau whose value decreases linearly with concentration (for $\phi < 0.3\%$). This confirms a central prediction for active pusher suspensions in the linear kinetic regime and validates the assumptions of the model, the main ones being the possibility to use the Bretherton Jeffery equations as a reliable swimming kinetic model and, most importantly, the hypothesis of the existence of an effective Gaussian disorientation noise, that eases the resolution of the Fokker-Planck equation. The most striking feature of the rheological response is indeed the emergence of a viscousless superfluidity regime ($\eta \sim 0$ or even lower). Presently, there is no *ab initio* microhydrodynamic calculation describing the impact of bacteria interactions and, possibly, the influence of collective organization on the macroscopic rheology. Therefore, one has to rely on phenomenological arguments to identify the possibly relevant macroscopic hydrodynamic contributions [2,23]. In this framework, several authors [23–25] investigated the responses to shear of active polar particles, and, remarkably, they predicted the possibility of a transition to a “zero-viscosity” regime when the activity is increased. This result can also be cast in the framework of recent experimental works pointing out the possible use of bacterial motion to

drive mechanical devices [31–33]. Actually, this Letter goes in this direction, as we show, at least in principle, that rotational macroscopic power could be extracted from the swimming activity as for a rotatory motor [25]. Finally, such a strong viscosity reduction may be a crucial element when considering macroscopic transport and particle dispersion in porous systems or in capillary networks, a central question to many applications involving bacterial fluids.

We acknowledge J.-P. Hulin, A. Lindner, A. Rousselet, and D. Salin for useful discussions and comments. This work is supported by a public grant from the Laboratoire d'Excellence Physics Atom Light Mater (LabEx PALM) overseen by the French National Research Agency (ANR) as part of the Investissements d'Avenir program (reference: ANR-10-LABX-0039).

*Corresponding author.

harold.auradou@u-psud.fr

- [1] D. L. Koch and G. Subramanian, *Annu. Rev. Fluid Mech.* **43**, 637 (2011).
- [2] M. C. Marchetti, J. F. Joanny, S. Ramaswamy, T. B. Liverpool, J. Prost, M. Rao, and R. Aditi Simha, *Rev. Mod. Phys.* **85**, 1143 (2013).
- [3] E. Lauga and T. R. Powers, *Rep. Prog. Phys.* **72**, 096601 (2009).
- [4] H. C. Berg, *E. coli in Motion* (Springer, New York, 2004).
- [5] Y. Hatwalne, S. Ramaswamy, M. Rao, and R. A. Simha, *Phys. Rev. Lett.* **92**, 118101 (2004).
- [6] J. Toner, Y. Tu, and Ramaswamy, *Ann. Phys. (Amsterdam)* **318**, 170 (2005).
- [7] X.-L. Wu and A. Libchaber, *Phys. Rev. Lett.* **84**, 3017 (2000).
- [8] A. Sokolov and I. S. Aranson, *Phys. Rev. Lett.* **103**, 148101 (2009).
- [9] S. Rafai, L. Jibuti, and P. Peyla, *Phys. Rev. Lett.* **104**, 098102 (2010).
- [10] K. C. Leptos, J. S. Guasto, J. P. Gollub, A. I. Pesci, and R. E. Goldstein, *Phys. Rev. Lett.* **103**, 198103 (2009).
- [11] G. Miño, T. E. Mallouk, T. Darnige, M. Hoyos, J. Dauchet, J. Dunstan, R. Soto, Y. Wang, A. Rousselet, and E. Clement, *Phys. Rev. Lett.* **106**, 048102 (2011).
- [12] C. Dombrowski, L. Cisneros, S. Chatkaew, R. E. Goldstein, and J. O. Kessler, *Phys. Rev. Lett.* **93**, 098103 (2004).
- [13] A. Sokolov, I. S. Aranson, J. O. Kessler, and R. E. Goldstein, *Phys. Rev. Lett.* **98**, 158102 (2007).
- [14] A. Sokolov and I. S. Aranson, *Phys. Rev. Lett.* **109**, 248109 (2012).
- [15] J. Dunkel, S. Heidenreich, K. Drescher, H. H. Wensink, M. Bär, and R. E. Goldstein, *Phys. Rev. Lett.* **110**, 228102 (2013).
- [16] J. Gachelin, G. Mino, H. Berthet, A. Lindner, A. Rousselet, and E. Clement, *New J. Phys.* **16**, 025003 (2014).
- [17] D. Saintillan and M. J. Shelley, *J. R. Soc. Interface* **9**, 571 (2012).
- [18] R. Rusconi, J. S. Guasto, and R. Stocker, *Nat. Phys.* **10**, 212 (2014).
- [19] B. M. Haines, A. Sokolov, I. S. Aranson, L. Berlyand, and D. A. Karpeev, *Phys. Rev. E* **80**, 041922 (2009).
- [20] D. Saintillan, *Exp. Mech.* **50**, 1275 (2010).
- [21] S. D. Ryan, B. M. Haines, L. Berlyand, F. Ziebert, and I. S. Aranson, *Phys. Rev. E* **83**, 050904(R) (2011).
- [22] M. Moradi and A. Najafi, *Europhys. Lett.* **109**, 24001 (2015).
- [23] M. E. Cates, S. M. Fielding, D. Marenduzzo, E. Orlandini, and J. M. Yeomans, *Phys. Rev. Lett.* **101**, 068102 (2008).
- [24] L. Giomi, T. B. Liverpool, and M. C. Marchetti, *Phys. Rev. E* **81**, 051908 (2010).
- [25] S. Fürthauer, M. Neef, S. W. Grill, K. Kruse, and F. Jülicher, *New J. Phys.* **14**, 023001 (2012).
- [26] J. Gachelin, G. Mino, H. Berthet, A. Lindner, A. Rousselet, and E. Clement, *Phys. Rev. Lett.* **110**, 268103 (2013).
- [27] J. Adler, *J. Bacteriol.* **92**, 121 (1966).
- [28] C. Douarche, A. Buguin, H. Salman, and A. Libchaber, *Phys. Rev. Lett.* **102**, 198101 (2009).
- [29] See Supplemental Material at <http://link.aps.org/supplemental/10.1103/PhysRevLett.115.028301> for (1) the variation of the viscosity η , of the mean bacteria velocity and diffusion coefficient with the oxygen concentration and (2) the details of the calculation to estimate the strength of the force dipole based on the rheological data.
- [30] J. Saragosti, P. Silberzan, and A. Buguin, *PLoS One* **7**, e35412 (2012).
- [31] Y. Hiratsuka, M. Makoto, T. Tetsuya, and U. Taro, *Proc. Natl. Acad. Sci. U.S.A.* **103**, 13618 (2006).
- [32] A. Sokolov, M. M. Apodaca, B. A. Grzybowski, and I. S. Aranson, *Proc. Natl. Acad. Sci. U.S.A.* **107**, 969 (2010).
- [33] R. Di Leonardo, L. Angelani, D. Dell'Arciprete, G. Ruocco, V. Iebba, S. Schippa, M. P. Conte, F. Mecarini, F. De Angelis, and E. Di Fabrizio, *Proc. Natl. Acad. Sci. U.S.A.* **107**, 9541 (2010).